Dalton Transactions

Accepted Manuscript

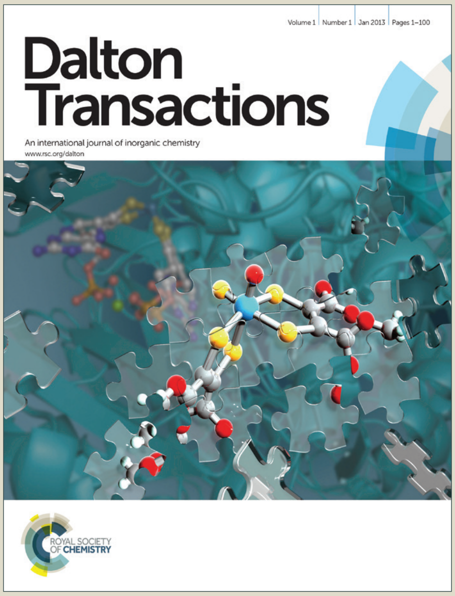

ROYAL SOCIETY OF CHEMISTRY

www.rsc.org/dalton

Redox Chemistry of Ruthenium ions in Mono-substituted Keggin Tungstophosphate: A New Synthetic Extension for Ruthenium Derivatives based on $[PW_{11}O_{39}Ru^{VI}N]^{4-}$

Bin Liu,[a] Jun Yan,*[a] Yi-Fang Wang,[a] Xiao-Yi Yi *[a]

[a] College of Chemistry and Chemical Engineering, Central South University, Changsha, Hunan 410083, P. R. China.
Fax: 86 731 88879616; Tel: 86 731 88879616;
E-mail: Yan, yanjun@csu.edu.cn; Yi, xyyi@csu.edu.cn

Abstraction

We herein report the synthesis and characterization of a series of ruthenium-substituted Keggin-type heteropolytungstates containing $\{Ru^{II}(NO)\}$, $\{Ru^{III}(H_2O)\}$ or $\{Ru^{IV}Cl\}$ species. Although anionic $[PW_{11}O_{39}Ru^{II}(NO)]^{4-}$ (**1**) and $[PW_{11}O_{39}Ru^{III}(H_2O)]^{4-}$ (**2**) are known, a new synthetic method for the preparation of $(n\text{-}Bu_4N)_4$[**1**] and $(n\text{-}Bu_4N)_4$[**2**] is developed in this paper. Treatment of $(n\text{-}Bu_4N)_4[XW_{11}O_{39}(Ru{\equiv}N)]$ with Me_3NO afforded ruthenium(II) nitrosyl complex $(n\text{-}Bu_4N)_4$[**1**] in almost quantitative yield. Photolysis of $(n\text{-}Bu_4N)_4$[**1**] solution in CH_3CN/H_2O gives $(n\text{-}Bu_4N)_4$[**2**], which are readily oxided by $PhICl_2$ to yield Ru^{IV} complex $(n\text{-}Bu_4N)_4[PW_{11}O_{39}Ru^{IV}Cl]$ ($(n\text{-}Bu_4N)_4$[**3**]). These complexes are fully characterized by ^1H NMR, ^{31}P NMR spectra, infrared spectra, cyclic voltammetry, element analysis, thermogravimetric-differential thermal analysis, electrospray ionization mass spectrometry (ESI-MS) spectra and X-ray photoelectron spectroscopy (XPS).

Introduction

Ruthenium-substituted polyoxometalates have received attention owing to their structural, redox, catalytic and magnetical properties.[1-4] Mono-lacunary Keggin type $[XW_{11}O_{39}]^{n-}$ (POM, X = P or Si), as a class of all-inorganic oxygen ligand, is capable of stabilizing ruthenium ions in various oxidation states. Numerous ruthenium-substituted mono-lacunary Keggin polyoxometalates have been investigated experimentally and theoretically, including Ru^{II} complexes $[XW_{11}O_{39}(RuL)]^{n-}$ (L = η^6-benzene, -pyridine,[5-6] -NH_3, -H_2O, -dimethyl sulfoxide (DMSO)[7-8,11a,11c] -NO,[9] -CO[10]), Ru^{III} complexes $[XW_{11}O_{39}(RuL)]^{n-}$ (L = -μ-O, -H_2O,[11,12] -DMSO,[12a] -pyridine,[13] -pyrazine,[14]), Ru^{IV} complexes $[XW_{11}O_{39}(RuL)]^{n-}$ [11a,15-17] and Ru^{VI} complexes $[PW_{11}O_{39}(Ru\equiv N)]^{4-}$.[18] The ruthenium center chelated in lacunary heteropolyoxotungstates has revealed unique redox properties. For example, ruthenium nitrido based on organic ligand reacts with PPh_3 produce a Ru^{IV} species,[19] however, analogous reaction based on $[XW_{11}O_{39}(Ru\equiv N)]^{4-}$ generate a Ru^{V} products.[20] Among these polyoxometalate compounds, most of the previously reported synthetic procedures are not always straightforward or limited to the low yield. For example, a few of synthetic approaches to the most common Ru^{III} precursor $[PW_{11}O_{39}Ru^{III}(H_2O)]^{4-}$ had been reported,[11] however, it seemed that there was not a standard procedure to afford it, usually suffered from complicated multi-step synthesis, strict reaction conditions and/or the need for extensive purification steps. In this regard, we decide to make efforts to investigate a facile approach to synthesize ruthenium-substituted Keggin-type heteropolyoxotungstates with high yield by easily controllable redox reaction.

Herein, We report the stepwise synthesis and characterization of a series of ruthenium-substituted tungstophosphate derivatives based on $[PW_{11}O_{39}(Ru\equiv N)]^{4-}$ precursor, including Ru(II)-nitrosyl $(n\text{-}Bu_4N)_4[PW_{11}O_{39}Ru^{II}(NO)]$ ($(n\text{-}Bu_4N)_4[\mathbf{1}]$), Ru(III)-aqu $(n\text{-}Bu_4N)_4[PW_{11}O_{39}Ru^{III}(H_2O)]$ ($(n\text{-}Bu_4N)_4[\mathbf{2}]$) and Ru(IV) complex $(n\text{-}Bu_4N)_4[PW_{11}O_{39}Ru^{IV}Cl]$ ($(n\text{-}Bu_4N)_4[\mathbf{3}]$), as shown in Scheme 1. These complexes are fully characterized by ^{1}H-NMR, ^{31}P-NMR spectra, infrared spectra (IR), cyclic voltammetry (CV), element analysis (EA), thermogravimetric-differential thermal analysis (TGA), electrospray ionization mass spectrometry (ESI-MS) spectra and X-ray photoelectron spectroscopy (XPS).

Experimental Sections

General Considerations. ^1H NMR and ^{31}P NMR spectra were recorded on a Bruker AVANCEIII 500M spectrometer operating at 500 MHz and 202 MHz, and Chemical shifts (δ, ppm) were reported with reference to $SiMe_4$ and H_3PO_4, respectively. Infrared spectra (KBr) were recorded on nicolet 6700 spectrometer FT-IR spectrophotometer. UV-Vis spectra were recorded on Shimadzu UV-2600 spectrophotometer at ambient temperature with a 1 cm quarts cell. Elemental analyses for C, H and N were performed on a Perkin Elmer 240C elemental analyzer. Cyclic voltammetry were measured on CHI610E machine in an acetonitrile solution using a standard three-electrode cell. The working electrode is a glassy carbon electrode (diameter 3 mm), the reference electrode is a $Ag/AgNO_3$ (0.1 M in MeCN) and the counter electrode is a platinum wire. Thermogravimetric-differential thermal analysis was recorded on NETZSCH STA449C machine. X-ray photoelectron spectroscopic analysis was performed using a Kratos Axis 165 spectrometer (Kratos Analytical) with monochromatic Al Kα radiation (hν= 1486.71 eV). The pressure of the analysis chamber during experiments was less than 1×10^{-10} Torr. The beam current on the target was 1 μA with primary ion energy of 4 keV and a scanned area of 2×2 mm^2. The survey (wide) spectra were collected from 1100 to 0 eV with a pass energy of 160 eV, a step size of 0.35 eV and a dwell time of 150 ms on average over at least three scans. High-resolution spectra of the Ru 3d, W 4f, Cl 2p, O 1s, C 1s and N 1s were acquired with a pass energy of 40 eV and a dwell time of 300 ms on average over 16 scans. Nonlinear optimization of the Marquardt algorithm (Casa XPS) was used to determine the peak model parameters, such as peak positions, widths and intensities. The model peaks to describe XPS core-level lines for curve fitting were a product of Gaussian and Lorentzian functions. The spectrometer was calibrated by setting the C 1s binding energy at 284.7 eV. Complex $(n\text{-}Bu_4N)_4[PW_{11}O_{39}(Ru{\equiv}N)]$ were prepared according to literature methods.[18] All of other chemicals were obtained from J&K Scientific.

Preperation of $(n\text{-}Bu_4N)_4[PW_{11}O_{39}Ru^{II}(NO)]$ ($(n\text{-}Bu_4N)_4$[**1**]) To a green solution of $(n\text{-}Bu_4N)_4[PW_{11}O_{39}Ru{\equiv}N]$ (3000 mg, 0.80 mmol) in CH_3CN (100 mL) was added 1.2 equivalence of Me_3NO (74 mg, 1.0 mmol) in CH_3CN (2 mL). The reaction mixture was stirred for 8 h. Color of solution turned from green to brown. The solution was reduced to about 15 mL by *vacuum*, and ethyl ether (100 mL) was added slowly. Brown-yellow powder was precipitated, dried, and identified as (n-$Bu_4N)_4$[**1**]. Yield: 2910 mg (97.0 % based on amount of (n-$Bu_4N)_4[PW_{11}O_{39}Ru{\equiv}N]$). Brown block single crystal sample was afforded by slow evaporation of CH_3CN-H_2O solution of (n-$Bu_4N)_4$[**1**] in an open vial at room temperature. ^{31}P NMR (CD_3CN): δ (ppm) -14.34; IR (KBr, cm^{-1}): 502 (w), 592 (w), 663 (w), 805 (vs), 887 (s), 963 (s), 1038 (m), 1091 (s), 1153 (w), 1382 (w), 1481 (m), 1632 (w), 1850 (vs), 2872(s), 2930 (s), 2961 (vs), 3435 (br); UV–vis (CH_3CN) [λ_{max}, nm (ε, $M^{-1}cm^{-1}$)]: 213 (53575), 261 (50475). Cyclic voltammogram: $E_{1/2}$ = 951 mV (reversible); $E_{1/2}$ = -684 mV (reversible) vs Ag/$AgNO_3$ (0.1 M in MeCN); Anal. Calcd for $C_{64}H_{144}N_5PW_{11}O_{40}Ru$: C, 20.34; H, 3.84; N, 1.85. found: C, 20.33; H, 4.08; N, 1.90

Preperation of (n-$Bu_4N)_4[PW_{11}O_{39}Ru^{III}(H_2O)]$ ((n-$Bu_4N)_4$[**2**]) A solution of (n-$Bu_4N)_4$[**1**] (40 mg, 0.01 mmol) in CH_3CN (8 mL) was irradiated with a Hg immersion lamp (253.7 nm, 70 W) for 3 h, of which color changed from brown to brown-red. The solvent was reduced to about 1 mL by *vacuum*, and 2 mL ethyl ether was added slowly. Brown-red powder was precipitated, dried and identified as. (n-$Bu_4N)_4$[**2**]. Brown-red block single crystal sample was afforded by slow evaporation of CH_3CN-H_2O solution of (n-$Bu_4N)_4$[**2**] at room temperature within one week. Yield: 38.2 mg (95.7 %). ^{31}P NMR (CD_3CN): δ (ppm) -72.8 (broad); IR (KBr, cm^{-1}): 512 (w), 624 (w), 798 (vs), 883 (s), 962 (s), 1048 (m), 1082 (s), 1153 (w), 1382 (m), 1481 (m), 1631 (m), 2872 (s), 2932 (s), 2961 (vs), 3436 (br); UV–vis (CH_3CN) [λ_{max}, nm (ε, $M^{-1}cm^{-1}$)]: 213 (48075), 260 (34650). Cyclic voltammogram: $E_{1/2}$ = 1399 mV (reversible); $E_{1/2}$ = 542 mV (reversible); $E_{1/2}$ = -688 mV) (reversible) vs Ag/$AgNO_3$ (0.1 M in MeCN); Anal. Calcd for $C_{66}H_{147}N_5PW_{11}O_{39}Ru{\cdot}CH_3CN$: C, 21.32; H, 3.95; N, 2.19. found: C, 21.07; H, 4.14; N, 2.13

Preperation of (n-$Bu_4N)_4[PW_{11}O_{39}Ru^{IV}(Cl)]$ ((n-$Bu_4N)_4$[**3**]) Mixtures of (n-$Bu_4N)_4$[**2**] (40 mg, 0.01 mmol) and freshly prepared $PhICl_2$ (5.5mg, 0.02mmol) in CH_3CN (4 mL) was stirred for 2 h, of which color changed from brown-red to red within 10 min. The solution was filtered. Filtrate was reduced to about 1 mL, and layered by ether to afford the darkish red block crystals. Yield: 37.5 mg (93.3%). ^{31}P

NMR δ (ppm) -15.06. IR (KBr, cm^{-1}): 512 (w), 804 (vs), 883 (s), 963 (s), 1045 (m), 1080 (s), 1153 (w), 1381 (m), 1481 (m), 1634 (m), 2872 (s), 2927 (s), 2961 (vs), 3435 (br). UV–vis (CH_3CN) [λ_{max}, nm (ε, $M^{-1}cm^{-1}$)]: 210 (45400), 260 (33850). Cyclic voltammogram: $E_{1/2}$ = 1208 mV (irreversible); $E_{1/2}$ = 287 mV (reversible); $E_{1/2}$ = -828 mV (irreversible) vs Ag/$AgNO_3$ (0.1 M in MeCN); Anal. calcd for $C_{64}H_{144}N_4PW_{11}O_{39}RuCl$: C, 20.32; H, 3.84; N, 1.48. found: C, 20.48; H, 4.09; N, 1.80.

Results and Discussion

Ruthenium-nitrosyl $(n\text{-}Bu_4N)_4$[**1**] and ruthenium-aqueous $(n\text{-}Bu_4N)_4$[**2**] have been the known complexes. Recently, *Sokolov* and coworkers reported treatment of $[Ru(NO)Cl_5]^{2-}$ and $[PW_{11}O_{39}]^{7-}$ under hydrothermal condition afforded $(n\text{-}Bu_4N)_4$[**1**], which reacted with both hydrazine and hydroxylamine to form $(n\text{-}Bu_4N)_4$[**2**].[9a] Several other reports on the preparation and structural characterization of $(n\text{-}Bu_4N)_4$[**2**] have also been described in the literature.[5a,9,11,12] In this study, a new procedure was found to synthesize these two complexes. Treatment of ruthenium nitrido $(n\text{-}Bu_4N)_4[PW_{11}O_{39}(Ru{\equiv}N)]$ with Me_3NO in CH_3CN readily afforded $(n\text{-}Bu_4N)_4$[**1**] (Scheme 1). Monitored by ^{31}P NMR, the reaction finished within 2h. Accompanying reactions, the color of reaction solution gradually changed from green to darkish brown, and the final isolated yield is almost quantitative. Irradiation of $(n\text{-}Bu_4N)_4$[**1**] in CH_3CN/H_2O with UV light at room temperature readily gave the ruthenium aqueous complex $(n\text{-}Bu_4N)_4$[**2**] with yield up to 95.7 %. It is worth noting that the formation of CH_3CN complex **2** is possible, because there are two CH_3CN molecules based on the elemental analysis of solid **2** despite no CH_3CN bands according to its IR spectrum. The previous report has reported that Ru^{III} aqueous $(n\text{-}Bu_4N)_4$[**2**] shows two well-defined reversible redox pairs attributed to $Ru^{III/II}$ and $Ru^{IV/III}$.[9a] It is proved to be a convenient starting material for Ru^{II} and Ru^{IV} complexes. Further, the oxidation reaction of $(n\text{-}Bu_4N)_4$[**2**] with $PhICl_2$ in CH_3CN for 2 h afforded darkish red $(n\text{-}Bu_4N)_4$[**3**]. The isolated yield reach 93.3 %. Complexes $(n\text{-}Bu_4N)_4$[**1**], $(n\text{-}Bu_4N)_4$[**2**] and $(n\text{-}Bu_4N)_4$[**3**] show significant difference in color (Fig. S1), could be isolated as block crystals by slow evaporation of $CH_3CN\text{-}H_2O$ solution in an open vial at room temperature, which are suitable for X-ray diffraction. However, the single crystal structure analysis is not suitable due to the disordering of highly symmetric mono-metal-substituted Keggin-type heteropolyoxotungstates. They belong to the cubic crystallographic system (a = 17.52(4) Å, V = 5375(12) Å^3) for (n-Bu$_4$N)$_4$[**3**]. Thus, (n-Bu$_4$N)$_4$[**3**] as well as (n-Bu$_4$N)$_4$[**1**], (n-Bu$_4$N)$_4$[**2**] are fully characterized by ^{1}H-NMR, ^{31}P-NMR spectra, infrared spectroscopy (IR), cyclic voltammetry (CV), element analysis (EA), thermogravimetric-differential thermal analysis (TGA), electrospray ionization mass spectrometry (ESI-MS) spectra and X-ray photoelectron spectroscopy (XPS). In this paper (n-Bu$_4$N)$_4$[**1**] and (n-Bu$_4$N)$_4$[**2**] were confirmed by IR, NMR, ESI-MS and EA according to the literature.

During the synthesis of (n-Bu$_4$N)$_4$[**2**], the ^{31}P-NMR was measured to monitor this photolysis reaction (Fig. S2). It was found new broad peak (-72.8 ppm) and sharp peaks (-13.1 ppm, -11.2 ppm and -15.0 ppm) appeared during the irradiation experiment. Broad peak corresponds to the paramagnetic (n-Bu$_4$N)$_4$[**2**] as final product (Fig. 1). This peak grew simultaneously with the decrease in the intensity of the signal corresponding to starting (n-Bu$_4$N)$_4$[**1**]. Other sharp peaks due to the diamagnetic as intermediates started to vanish after disappearance of starting compound. The identity of these intermediates could not be unequivocally determined on the basis of only ^{31}P NMR spectra yet, and the analogous diamagnetic intermediates also appeared in the formation of (n-Bu$_4$N)$_4$[**2**] through the reaction of (n-Bu$_4$N)$_4$[**1**] with both hydrazine and hydroxylamine.[9] The ^{31}P NMR spectrum of (n-Bu$_4$N)$_4$[**3**] in CD$_3$CN is also studied. As shown in Fig. 1, the Ru in compound (n-Bu$_4$N)$_4$[**3**] is clearly diamagnetic, identified by its sharp ^{31}P NMR signal at -15.06 ppm. That is similar to what observed for (n-Bu$_4$N)$_4$[**1**] and starting (n-Bu$_4$N)$_4$[XW$_{11}$O$_{39}$(Ru≡N)] (-14.34 ppm and -15.05 ppm in CD$_3$CN, respectively), and is significantly different from paramagnetic (n-Bu$_4$N)$_4$[**2**] (broad peak at -72.8 ppm in CD$_3$CN). As a result, it could rule out the existence of paramagnetic Ru^{III} and Ru^{V} in the solution, and the oxidation state of Ru in (n-Bu$_4$N)$_4$[**3**] is expected as Ru^{IV}, which is further confirmed by the XPS spectrum. Fig. 2 displays the Ru 3d core level spectra measured from **1-3** and (n-Bu$_4$N)$_4$[PW$_{11}$O$_{39}$(Ru^{VI}≡N). The fitting model used consisted of Lorentzian-Gaussian peak functions. The C$_{1S}$ spectrum from C-H and C-N in n-Bu$_4$N$^+$ taken under identical conditions is also shown for comparison. The spectra consist of the Ru 3d$_{5/2}$ and Ru 3d$_{3/2}$ peaks appearing as a result of a spin-orbital splitting. It is reasonable to assume the presence of ruthenium in a single valence state. The binding energy values of the Ru 3d$_{5/2}$ and Ru 3d$_{3/2}$ core level for

1-3 gradually increases as the oxidation state of the ruthenium increases, in order of $(n\text{-}Bu_4N)_4[PW_{11}O_{39}(Ru^{VI}\equiv N)$ > $(n\text{-}Bu_4N)_4$[**3**] > $(n\text{-}Bu_4N)_4$[**2**] > $(n\text{-}Bu_4N)_4$[**1**], thereby, indicating the oxidation state of Ru in **3** is higher than that in **2**, and lower than that in $[PW_{11}O_{39}(Ru\equiv N)]^{4-}$, to reach IV.[21] Furthermore, Cl $2p_{1/2}$ and Cl $2p_{3/2}$ peaks in **3** indicate the presence of the elements chloride (Fig. S3).

To further confirm these structures, the ESI-MS technique had been applied for characterization of cluster,[22] as shown in Fig. S4. Although the mass spectrometry did not provide information about the initial net charge of the ligated complex because redox inter-conversion is ubiquitous during the ESI process, it can clearly show the Ru/W ratio and the $\{PW_{11}O_{39}Ru\}$ framework.[23] The negative high resolution ESI mass spectrum of acetonitrile solutions of **1** reveals the presence of intact triply charged [**1**+H]$^{3-}$ and [**1**+TBA]$^{3-}$ species accompanied by doubly charged [**1**+2H]$^{2-}$, [**1**+H+TBA]$^{2-}$ and [**1**+2TBA]$^{2-}$ peaks, which is consist with the previously report ESI-MS data of this cluster.[9] The mass spectrum of acetonitrile solutions of **2** show that the coordinated H_2O at the Ru site has been liberated under collision induced dissociation (CID) condition.[24] All the main peaks can be assigned as dehydrate cluster $[PW_{11}O_{39}Ru^{III}]$ with a handful H^+ and TBA^+ cations. Unexpectedly, all the main peaks consist the formula of $\{H_n(TBA)_m[PW_{11}O_{39}Ru^{IV}(H_2O)]\}^{3-/2-}$ (n+m = 1 or 2) when **3** is examined under the same condition but no peak can be reasonably assigned as $[PW_{11}O_{39}Ru^{IV}Cl]$ related species, which indicate the Cl^- ligand has been exchanged by H_2O during the ESI process. Compare to the MS of **2**, the higher oxidation of Ru on the cluster **3** enhanced the Ru-OH$_2$ bonding. Additionally, **1** and **2** characterized by IR as well. The IR spectrum (Fig. 3) in $(n\text{-}Bu_4N)_4$[**3**] shows about ν = 2961, 2930, 2872 cm^{-1} and 1080, 1040 cm^{-1} bands attributed to the TBA and P-O stretching frequency. The characteristic bands of $(n\text{-}Bu_4N)_4$[**3**] for W-O of the Keggin structure in the low-frequency region are only slightly shifted with respect to $(n\text{-}Bu_4N)_4$[**1**] and $(n\text{-}Bu_4N)_4$[**2**], and the UV-Vis (Fig. S5) absorption bands $(n\text{-}Bu_4N)_4$[**3**] is also very similar with that of $(n\text{-}Bu_4N)_4$[**1**] and $(n\text{-}Bu_4N)_4$[**2**] in terms of peak positions and peak intensities. It suggests the framework of complex **3** are similar with that of **1** and **2.**

The electrochemical behavior of $(n\text{-}Bu_4N)_4$[**1**]-$(n\text{-}Bu_4N)_4$[**3**] were measured in CH_3CN solution, as shown in Fig. 4. Similar to the previously reported Ru^{II}-NO analogous, two reversible redox pairs ($E_{1/2}$ = 951mV and -684mV) were observed in (n-$Bu_4N)_4$[**1**]. The $E_{1/2}$ = 951mV versus Ag/$AgNO_3$ belongs to the $Ru^{III/II}$ couple. The redox of (n-$Bu_4N)_4$[**2**] waves in the positive region ($E_{1/2}$ = 542mV and 1399mV versus Ag/$AgNO_3$) are attributed to $Ru^{III/II}$ and $Ru^{IV/III}$ couples, respectively. Complex (n-$Bu_4N)_4$[**3**] exhibited one reversible redox ($E_{1/2}$ = 287mV versus Ag/$AgNO_3$) and one irreversible wave ($E_{1/2}$ =1208mV, versus Ag/$AgNO_3$), which are tentatively attributed to the $Ru^{IV/III}$ and $Ru^{V/IV}$ couples, respectively. No $Ru^{V/IV}$ oxidation was found up to 1.2 V. The redox process at negative position for **1**-**3** is detected and corresponds to the reduction of W^{VI} atoms. That is well compared to what found in mono-metal-substituted Keggin-type heteropolytungstates.[25]

As shown in Fig. S6, TGA for (n-$Bu_4N)_4$[**1**] and (n-$Bu_4N)_4$[**2**] display very similar behavior. Dehydration step is followed by decomposition. The weight losses 0.97 % for (n-$Bu_4N)_4$[**1**] and 1.81 % for (n-$Bu_4N)_4$[**2**]) up to 120-220 °C are due to bound solvent molecules. The thermogravimetric profiles of (n-$Bu_4N)_4$[**3**] in terms of solvent loss is flatter than that of (n-$Bu_4N)_4$[**1**] and (n-$Bu_4N)_4$[**2**]. There are almost not any weight loss below 180 °C. A sharp weight losses from 300 to 430 °C (16.37% for (n-$Bu_4N)_4$[**1**], 15.04 % for (n-$Bu_4N)_4$[**2**]), and from 180 to 430 °C (18.15% for (n-$Bu_4N)_4$[**3**]) are assigned to decomposition of the (n-$Bu_4N)^+$ cations, indicating (n-$Bu_4N)_4$[**1**] and (n-$Bu_4N)_4$[**2**] are stable until about 300 °C, while (n-$Bu_4N)_4$[**3**] starts to decompose at 180 °C.

Conclusion

In Summary, a new approach to ruthenium-substituted Keggin-type heteropolytungstates with almost quantitative yield was found. (n-$Bu_4N)_4[PW_{11}O_{39}(Ru{\equiv}N)$, as starting materials, supplies source of ruthenium and Keggin-type heteropolytungstate. This electrophilic ruthenium(VI) nitrido is readily reacted with Me_3NO to afford ruthenium(II)-nitrosyl (n-$Bu_4N)_4$[**1**]. This method has the advantage of high yield, short reaction time and simple in operation compared with hydrothermal reaction reported by *Sokolov* and coworkers. The nitrosyl group in (n-$Bu_4N)_4$[**1**] can be easily removed under irradiation with UV lamp to form ruthenium(III)-aqueous complex (n-$Bu_4N)_4$[**2**] in H_2O/MeCN solution. It may be considered as an alternative efficient route to prepare ruthenium(III) aqueous complex, which usually serves as common precursor of novel ruthenium polyoxometalates. (n-$Bu_4N)_4$[**2**]) is readily oxided by $PhICl_2$ to afford ruthenium(IV) (n-$Bu_4N)_4$[**3**]. All of these three complexes are fully characterized. Given the applications of ruthenium-substituted polyoxometalates in redox catalysis, Ru(IV) complex (n-$Bu_4N)_4$[**3**] are anticipated to display putative catalytic activity, such as water oxidation. Further research is under way.

Acknowledgment

This work was supported by the National Natural Science Foundation of China (proiect 21441006 and 21301194), and the Open-End Fund for the Valuable and Precision Instruments of Central South University.

References

1 M. T. Pope, *Heteropoly and Isopoly Oxometalates ed.*, Springer-Verlag, Berlin, 1983.

2 (a) C. L. Hill, Special thematic issue on polyoxometalates, *Chem. Rev.*, 1998, **98**, 1. (b) C. L. Hill and C. M. Prosser-McCartha, *Coord. Chem. Rev.*, 1995, **143**, 407.

3 (a) M. Sadakane and E. Steckhan, *Chem. Rev.*, 1998, **98**, 219. (b) N. Mizuno, K. Yamaguchi and K. Kamata, *Coord. Chem. Rev.* 2005, **249**, 1944. (c) J. J. Borrás-Almenar, E. Coronado, A. Muller, M. T. Pope, *Polyoxometalate Molecular Science*, Kluwer, Dordrecht, 2004.

4 (a) A. M. Khenkin and R. Neumann, *J. Am. Chem. Soc.*, 2008, **130**, 14474. (b) A. Yokoyama, K. Ohkubo, T. Ishizuka, T. Kojima and S. Fukuzumi, *Dalton Trans.*, 2012, **41**, 10006. (c) A. Proust, R. Thouvenot and P. Gouzerh, *Chem. Commun.*, 2008, 1837. (d) A. M. Khenkin, I. Efremenko, L. Weiner, J. M. L. Martin and R. Neumann, *Eur. J. Chem.*, 2010, **16**, 1356.

5 (a) S. Ogo, M. Miyamoto, Y. Ide, T. Sano and M. Sadakane, *Dalton Trans.,* 2012, **41**, 9901. (b) N. H. Nsouli, E. V. Chubarova, R. Al-Oweini, B. S. Bassil, M. Sadakane and U. Kortz, *Eur. J. Inorg. Chem.*, 2013, **10**, 1742.

6 S. Ogo, S. Moroi, T. Ueda, K. Komaguchi, S. Hayakawa, Y. Ide, T. Sano and M. Sadakane, *Dalton Trans.*, 2013, **42**, 7190.

7 (a) C. G. Liu, X. H. Guan, *Mol. Phys*., 2013, **111**, 3733. (b) A. Sartorel, P. Miró, M. Carraro, S. Berardi, O. Bortolini, A. Bagno, C. Bo and M. Bonchio, *Chem. Eur. J*, 2014, **20**, 10932.

8 (a) D. Laurencin, R. Thouvenot, K. Boubekeur, P. Gouzerh and A. Proust, *C. R. Chim*., 2012, **15**, 135. (b) A. Bagno, M. Bonchio, A. Sartorel, G. Scorrano, *Eur. J. Inorg. Chem.*, 2000, 17.

9 (a) M. N. Sokolov, S. A. Adonin, D. A. Mainichev C. Vicent, N. B. Kompankov, A. L. Gushchin, V. A. Nadolinny and V. P. Fedin, *Inorg. Chem*., 2013, **52**, 9675. (b) K. Filipek, *Inorg. Chim. Acta*, 1995, **231**, 237.

10 (a) M. Sadakane, Y. Iimuro, D. Tsukuma, B. S. Bassil, M. H. Dickman, U. Kortz, Y. Zhang, S. Ye and W. Ueda, *Dalton Trans*., 2008, 6692. (b) C. Vicent, S. A. Adonin, A. V. Anyushin, D. A. Mainichev and M. N. Sokolov, *Eur. J. Inorg. Chem*., 2014, 5618.

11 (a) C. Rong and M. T. Pope, *J. Am. Chem. Soc.*, 1992, **114**, 2932. (b) J. C. Bart and F. C. Anson, *J. Electroanal. Chem.*, 1995, **390**, 11. (c) K. Yamaguchi and N. Mizuno, *New J. Chem.* 2002, **26**, 972. (d) M. Sadakane and M. Higashijima, *Dalton Trans.*, 2003, 659.

12 (a) M. Sadakane, D. Tsukuma, M. H. Dickman, G. Bassil, U. Kortz, M. Higashijima and W. Ueda, *Dalton Trans.*, 2006, 4271. (b) M. S. S. Balula, I. C. M. S. Santos, J. A. F. Gamelas, A. M. V. Cavaleiro, N. Binsted and W. Schlindwein, *Eur. J. Inorg. Chem.*, 2007, 1027. (c) C. Besson, S. Chen, R. Villanneau, G. Izzet and A. Proust, *Inorg. Chem. Commun.*, 2009, **12**, 1042. (d) M. Murakami, D. Hong, T. Suenobu, S. Yamaguchi, T. Ogura and S. Fukuzumi, *J. Am. Chem. Soc*., 2011, **133**, 11605. (e) M. Sadakane, D. Tsukuma, M. H. Dickman, B. S. Bassil, U. Kortz, M. Capron and W. Ueda, *Dalton Trans.*, 2007, 2833. (f) S. Ogo, N. Shimizu, T. Ozeki, Y. Kobayashi, Y. Ide, T. Sano and M. Sadakane, *Dalton Trans.*, 2013, **42**, 2540.

13 M. Sadakane, S. Moroi, Y. Iimuro, N. Izarova, U. Kortz, S. Hayakawa, K. Kato, S. Ogo, Y. Ide, W. Ueda and T. Sano, *Chem. Asian. J.*, 2012, **7**, 1331.

14 J. C. Bart and F. C. Anson, *J. Electroanal. Chem*., 1995, **390**, 11.

15 Y. P. Liu, S. X. Guo, A. M. Bond, J. Zhang, Y. V. Geletii, C. L. Hill, *Inorg. Chem.*, 2013, **52**, 11986.

16 C. G. Liu, W. Guan, L. K. Yan and Z. M. Su, *Dalton Trans.*, 2011, **40**, 2967.

17 S. W. Chen, R. Villanneau, Y. L. Li, L. M. Chamoreau, K. Boubekeur, R. Thouvenot, P. Gouzerh and A. Proust, *Eur. J. Inorg. Chem.*, 2008, **13**, 2137.

18 (a) V. Lahootun, C. Besson, R. Villanneau, F. Villain, L. M. Chamoreau, K. Boubekeur, S. Blanchard, R. Thouvenot and A. Proust, *J. Am. Chem. Soc.*, 2007, **129**, 7127. (b) C. G. Liu, W. Guan, L. K. Yan, P. Song and Z. M. Su, *Dalton Trans.*, 2009, 6208.

19 H. F. Ip, X. Y. Yi, W. Y. Wong, I. D. Williams and W. H. Leung, *Dalton Trans.*, 2011, **40**, 11043.

20 C. Besson, Y. V. Geletii, F. Villain, R. Villanneau, C. L. Hill and A. Proust, *Inorg. Chem.*, 2009, **48**, 9436.

21 J. A. F. Gamelas, H. M. Carapuça, M. S. Balula, D. V. Evtuguin, W. Schlindwein, F. G. Figueiras, V. S. Amaral and A. M. V. Cavaleiro, *Polyhedron*, 2010, **29**, 3066.

22 (a) H. N. Miras, E. F. Wilson and L. Cronin, *Chem. Commun.* 2009, 1297. (b) P. Putaj, F. Lefebvre, *Coord. Chem. Rev.*, 2011, **255**, 1642. (c) N. V. Izarova, M. T. Pope, U. Kortz, *Angew. Chem. Int. Ed.*, 2012, **51**, 9492.

23 (a) M. N. Sokolov, S. A. Adonin, P. L. Sinkevich, C. Vicent, D. A. Mainichev and V. P. Fedin, *Dalton Trans.*, 2012, **41**, 9889. (b) M. T. Ma, T. Waters, K. Beyer, R. Palamarczuk, P. J. S. Richardt, R. A. J. O'hair and A. G. Wedd, *Inorg. Chem.*, **48**, 598.

24 (a) L. Vilà-Nadal, S. G. Mitchell, D. L. Long, A. Rodríguez-Fortea, X. López, J. M. Poblet and L. Cronin, *Dalton Trans.*, 2012, **41**, 2264. (b) S. Romo, N. S. Antonova, J. J. Carbó and J. M. Poblet, *Dalton Trans.*, 2008, 5166. (c) M. N. Sokolov, S. A. Adonin, P. L. Sinkevich, C. Vicent, D. A. Mainichev and V. P. Fedin, *Z. Anorg. Allg. Chem.*, 2014, **640**, 122.

25 (a) M. Sadakane, N. Rinn, S. Moroi, H. Kitatomi, T. Ozeki, M. Kurasawa, M. Itakura, S. Hayakawa, K. Kato, M. Miyamoto, S. Ogo, Y. Ide and T. Sano, *Z. Anorg.

Allg. Chem., 2011, **637**, 1467. (b) M. N. Sokolov, S. A. Adonin, D. A. Mainichev, C. Vicent, N. F. Zakharchuk, A. M. Danilenko and V. P. Fedin, *Chem. Commun*, 2011, **47**, 7833.

Scheme 1 The syntheses of (n-Bu$_4$N)$_4$[**1**], (n-Bu$_4$N)$_4$[**2**] and (n-Bu$_4$N)$_4$[**3**]

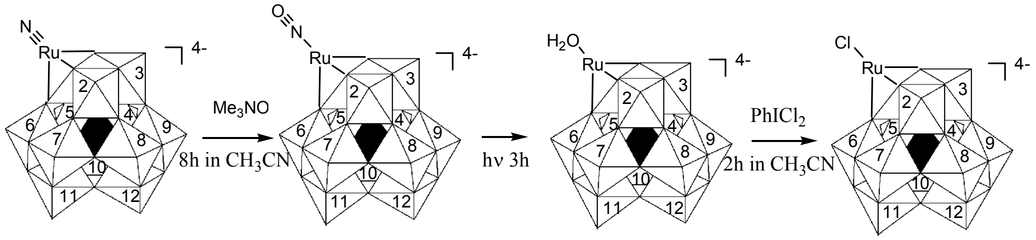

1 (97.0 %) **2** (95.7 %) **3** (93.3 %)

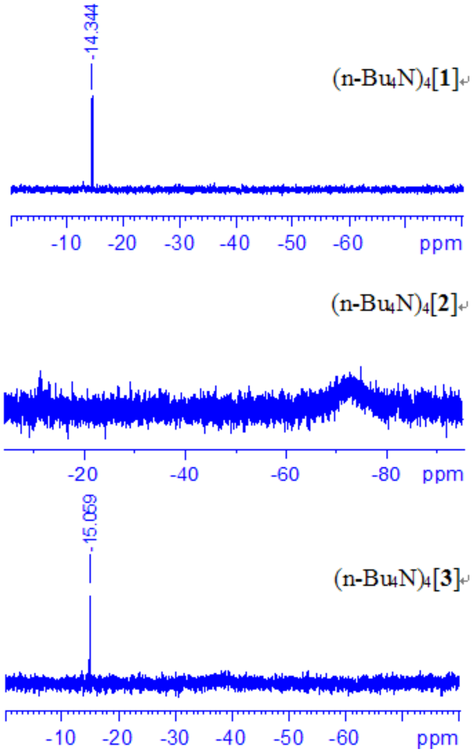

Fig. 1 the ^{31}P NMR of (n-Bu$_4$N)$_4$[**1**], (n-Bu$_4$N)$_4$[**2**] and (n-Bu$_4$N)$_4$[**3**] in CD$_3$CN.

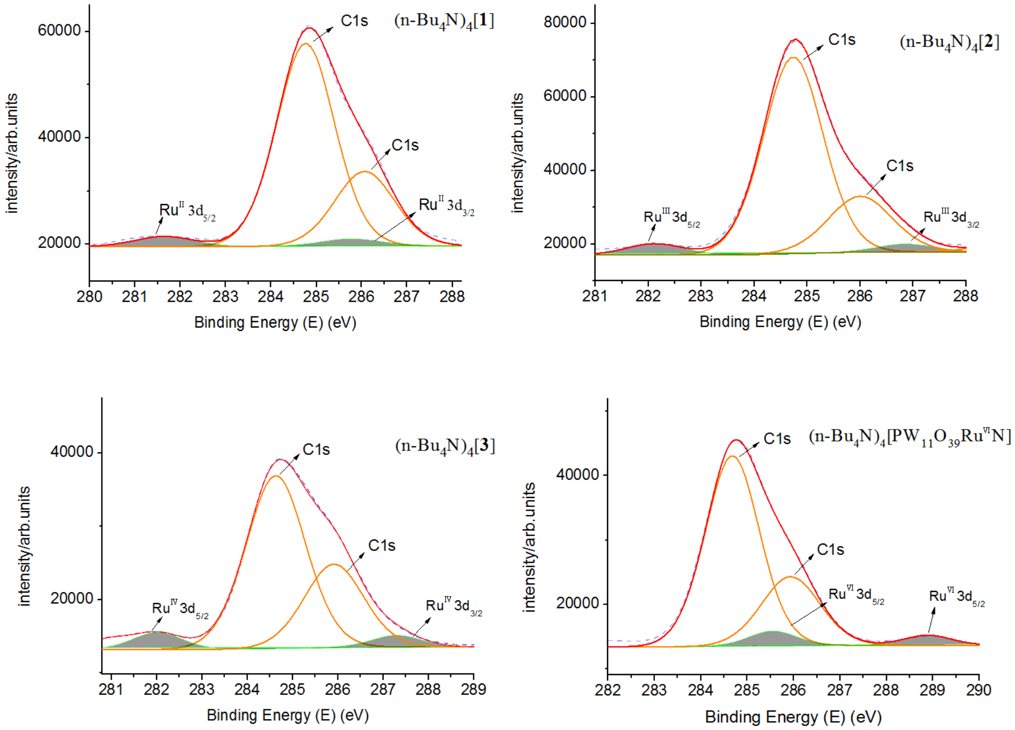

Fig. 2 X-ray photoelectron spectra for C 1s and Ru 3d. Peak deconvolution of the Ru 3d core-level energy region yields two ruthenium intensities at 281.6 eV ($3d_{5/2}$) and 285.8 eV ($3d_{3/2}$) for $(n\text{-}Bu_4N)_4[\mathbf{1}]$, 282.0 eV ($3d_{5/2}$) and 286.6 eV ($3d_{3/2}$) for $(n\text{-}Bu_4N)_4[\mathbf{2}]$, 282.0 eV ($3d_{5/2}$) and 287.2 eV ($3d_{3/2}$) for $(n\text{-}Bu_4N)_4[\mathbf{3}]$, 285.4 eV ($3d_{5/2}$) and 289.1 eV ($3d_{3/2}$) for $(n\text{-}Bu_4N)_4[PW_{11}O_{39}Ru^{VI}N]$ and carbon from TBA and graphitic carbon intensity at 284.7 eV and 286.1 eV, respectively.

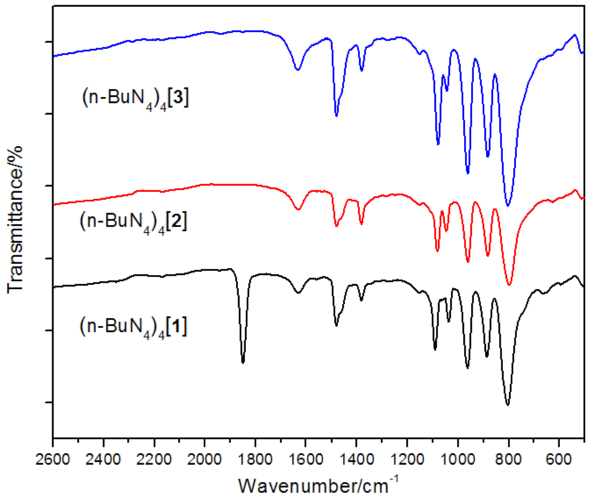

Fig. 3 Infrared spectrum of (n-$Bu_4N)_4$[**1**], (n-$Bu_4N)_4$[**2**] and (n-$Bu_4N)_4$[**3**]

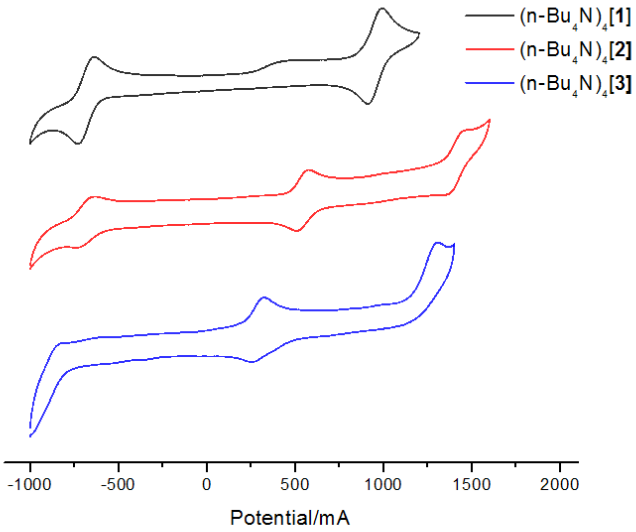

Fig. 4 Cyclic voltammogram of (n-Bu$_4$N)$_4$[**1**], (n-Bu$_4$N)$_4$[**2**] and (n-Bu$_4$N)$_4$[**3**] in acetonitrile with 0.1M TBABF$_4$ as supporting electrolyte versus Ag/AgNO$_3$ (scan rate 100 mV s^{-1})

A facile approach to ruthenium-substituted Keggin-type heteropolyoxotungstates with high yield by easily controllable redox reaction is described.

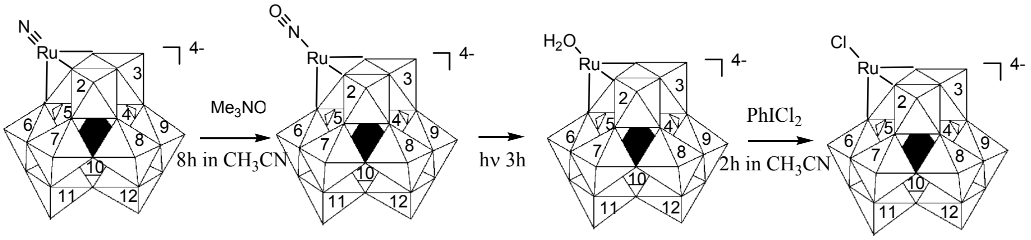

1 (97.0 %) **2** (95.7 %) **3** (93.3 %)